Nanoscale

COMMUNICATION

Boosting the oxidase mimicking activity of nanoceria by fluoride capping: rivaling protein enzymes and ultrasensitive F^- detection

Received 00th January 20xx,
Accepted 00th January 20xx

DOI: 10.1039/x0xx00000x

www.rsc.org/

Biwu Liu, Zhicheng Huang, and Juewen Liu*

Nanomaterial-based enzyme mimics (nanozymes) are currently a new forefront of chemical research. However, the application of nanozymes is limited by its low catalytic activity and low turnover numbers. Cerium dioxide nanoparticles (nanoceria) is among the few with oxidase activity. Herein, we report an interesting finding addressing its limitations. The oxidase activity of nanoceria is improved by over 100-fold by fluoride capping, rendering it more close to real oxidases (*e.g.*, cytochrome P450). The turnover number reached 700 in 15 min, drastically improved from ~15 turnovers for the naked particles. The mechanism is attributed to surface charge modulation and facilitated electron transfer by F^- capping based on ζ-potential and free radical measurement. Ultrasensitive sensing of fluoride was achieved with a detection limit of 0.64 μM F^- in water and in toothpastes, while no other tested anions can achieve the activity enhancement.

Developing nanomaterial-based enzyme mimics, known as nanozymes, is a new frontier in inorganic, materials and analytical chemistry.[1-7] Nanozymes are a subset of nanoparticle-based catalysts that catalyze enzyme-like reactions at ambient conditions. Nanozymes are attractive not only for their high stability and low-cost, but also for studying fundamental processes at nanoscale surfaces.[2] Many nanoparticles such as gold,[4,8,9] graphene oxide,[10,11] and various metal oxides[1,3,5,12-19] possess oxidase, peroxidase, and/or catalase like activities. It is interesting to note that while many peroxidase nanozymes were reported (*i.e.*, using H_2O_2 as a co-substrate), very few have oxidase activity.[9,19-23] The best known examples are gold nanoparticles for glucose oxidation,[9] and CeO_2 nanoparticles (nanoceria) that oxidize a diverse range of substrates.[20] Oxidase nanozymes are important since they do not require unstable H_2O_2 as a co-substrate.

Department of Chemistry, Waterloo Institute for Nanotechnology, University of Waterloo, Waterloo, Ontario, N2L 3G1, Canada
E-mail: liujw@uwaterloo.ca; Fax: +1 519 746 0435; Tel: +1 519 888 4567 ext. 38919

†.Electronic Supplementary Information (ESI) available: Methods, TMB oxidation kinetics and control experiments. See DOI: 10.1039/x0xx00000x

Nanoceria is a versatile nanozyme, displaying oxidase,[16,20] catalase,[24,25] superoxide dismutase,[26,27] and phosphatase[28] activities under different conditions. In 2009, Asati and co-workers first reported the oxidase-like activity of nanoceria.[20] Since then, nanoceria has become an attractive system receiving extensive studies. The catalytic activities of nanoceria were attributed to the mixed oxidation states of Ce^{3+} and Ce^{4+}, and related oxygen vacancies.[29,30] The role of redox states,[24] surface coating,[20] pH,[31] buffer composition,[32] and nucleotide triphosphate[16] were investigated. We hypothesize that surface chemistry plays a critical role in modulating substrate/product adsorption and electron transfer, thus influencing catalytic efficiency. A challenge in the nanozyme field is poor catalytic activity and low turnover, which is in sharp contrast to their highly efficient protein counterparts.

Fluoride (F^-) is critical in many biological, medical, and environmental applications.[33] From the chemistry standpoint, F^- as a hard Lewis base might adsorb strongly on nanoceria, since cerium is a hard Lewis acid. Adsorption of highly electron negative F^- can modulate the intrinsic energy bands of nanomaterials.[34-39] In this study, we aim to use nanoceria as a model to engineer a robust oxidase by exploring its surface chemistry, and we report an excellent nanozyme performance enabled by simple fluoride capping (Figure 1A).

Our nanoceria has an average size of ~5 nm by transmission electron microscopy (TEM) and dynamic light scattering (DLS) (Figure 1B). To study the oxidase activity of nanoceria, we first used 2,2'-azinobis(3-ethylbenzothiozoline)-6-sulfonic acid (ABTS) as the substrate. ABTS is colorless in water (inset of Figure 1C). After adding a low concentration of nanoceria, only a slight green color was observed, indicating oxidation of a small fraction of ABTS. Note that the color changed more with a higher concentration of nanoceria (data not shown). Surprisingly, with 1 mM F^-, the nanoceria quickly produced a deep green color. F^- is not an oxidizing agent and indeed mixing F^- with ABTS resulted in no color change. Therefore, F^- served as a promoter for nanoceria. We measured the UV-vis spectra of these samples (Figure 1C). Oxidized ABTS has a broad absorption feature peaked at 420 nm. This peak height is ~15-fold higher with F^- than without it. We also examined the oxidation of another

commonly used chromgenic substrate, 3,3',5,5'-tetramethylbenzidine (TMB) (Figure 1D). After F^- modification, nanoceria also exhibited enhanced oxidase-like activity. The peak at 652 nm is ~18-fold higher with F^- than without it. Therefore, the promoter effect of F^- is general for both negatively charged (ABTS) and positively charged (TMB) substrates.

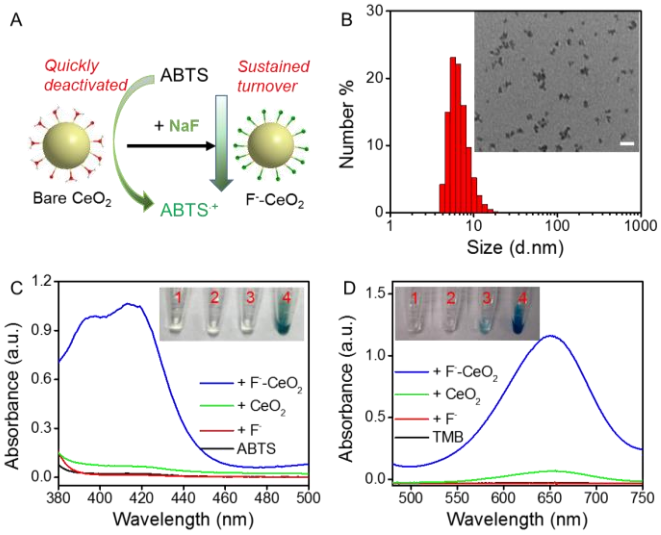

Figure 1. (A) A scheme showing F^--capped nanoceria with improved oxidase turnovers. (B) DLS size distribution and a TEM image (inset) of nanoceria. The scale bar in inset of (B) is 20 nm. UV-vis spectra of (C) ABTS (0.5 mM) and (D) TMB (1 mM) oxidation by nanoceria (100 μg/mL) with or without F^- (1 mM for ABTS, 5 mM for TMB) at pH 4 (acetate buffer, 20 mM) after 30 min of reaction. The insets are 1: the free substrate; 2: the substrate with F^-; 3: the substrate with bare CeO_2; 4: the substrate with F^--capped CeO_2. These samples were diluted 10 times for the UV-vis.

Next we performed steady-state kinetic assays at different substrate concentrations to extract enzyme parameters based on the initial reaction rates. Since the catalytic efficiency of nanoceria is much higher with F^-, we used 10-fold less nanoceria for the F^- containing samples to obtain a measurable rate. We fitted the data only in the first 30 sec for the initial fast phase (Figure 2). Just like real enzymes, a higher substrate concentration produced a faster rate, and saturated rates were reached at high substrate concentrations. Typical Michaelis-Menten curves were obtained. From these data, we made the double reciprocal plots (insets of Figure 2) to extract the Michaelis constant (K_m) and maximum initial reaction rate (V_{max}) (Table 1). Typically, a lower K_m value indicates a higher affinity between the enzyme and the substrate. After F^- modification, nanoceria shows higher affinities towards both ABTS (~3-fold decrease) and TMB (~10 fold decrease). The more pronounced binding improvement for TMB may be due to the inversed surface charge of nanoceria upon fluoride capping (*vide infra*). The V_{max} value of ABTS oxidation by F^--CeO_2 is only half of that by bare CeO_2. However, it should be noted that the concentration of F^--CeO_2 is 10-fold less than the bare CeO_2. The catalytic rate constant k_{cat} (V_{max}/[E]) values of nanoceria in the presence of F^- is ~5-fold higher compared to that in its absence for ABTS, and 10-fold for TMB. Overall, the catalytic efficiency, defined by k_{cat}/K_m, is ~15-fold higher with 0.5 mM F^- when ABTS was used as a substrate. The effect of F^- capping is even more significant when TMB is used as a substrate with ~ 100 folds increase of k_{cat}/K_m. Impressively, nanoceria after fluoride capping can rival natural oxidases (Table S1).

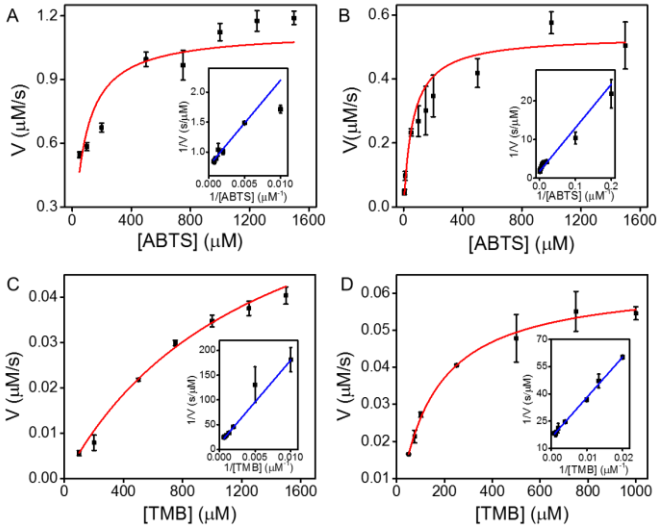

Figure 2. Steady-state kinetic assays of (A, C) bare CeO_2 (100 μg/mL, 430 nM) and (B, D) F^--capped CeO_2 (10 μg/mL, 43 nM) were carried out at pH 4 (acetate buffer, 20 mM). The concentration of (A, B) ABTS or (C, D) TMB was varied. The insets are the corresponding double reciprocal plots.

Table 1. A comparison of the steady-state enzyme kinetic parameters of bare nanoceria and F^- treated nanoceria (F^--CeO_2).

Sub	CeO_2 (nM)	V_{max}[a] (μM s^{-1})	K_m[b] (mM)	k_{cat}[c] (s^{-1})	k_{cat}/K_m (s^{-1} mM^{-1})
ABTS	430 (- F^-)	1.20	0.18	2.80	15.56
ABTS	43 (+ F^-)	0.55	0.062	12.84	207.10
TMB	430 (- F^-)	0.069	1.50	0.16	0.11
TMB	43 (+ F^-)	0.063	0.14	1.47	10.47

[a]: V_{max} is the maximal reaction velocity

[b]: K_m is the Michaelis constant

[c]: k_{cat} is the catalytic rate constant. k_{cat} = V_{max}/[E], and [E] is the concentration of nanoceria.

The steady-state kinetic parameters only reflect the initial stage of an enzymatic reaction. However, enzymes may be deactivated by product adsorption. The sustainability of an enzyme is as important as the initial reaction rate. Therefore, we examined the kinetics of ABTS and TMB oxidation. Without F^-, oxidation of ABTS was fast only in the first 30 sec, and then followed by a slow phase (Figure 3A, black trace and the inset). In this initial fast phase, only ~15 ABTS molecules were oxidized by each nanoceria. In the following 15 min, < 10 ABTS were converted. In the presence of 0.5 mM F^- (red trace), this biphasic behavior still occurred, but more ABTS were oxidized in the

first phase. With 1 mM F^-, the initial oxidation was slower compared to that with 0.5 mM F. However, the nanozyme was more robust and sustainable over a much longer time. After 15 min, ~700 ABTS were oxidized by each nanoceria. The turnover number reached 1200 ± 60 after overnight incubation (Figure S1). The effect of F^- on the initial rate enhancement is quite moderate for ABTS oxidation. The main role of F^- here is to make the catalyst more sustainable.

A key feature of enzymes is catalytic turnover. The quick deactivation of the bare nanozyme might be due to a tight adsorption of the oxidation product, inhibiting binding of new substrates. Fluoride capping has solved this problem. If we compare the turnover rates after the first minute, the 1 mM F^- sample was ~130-fold faster. Therefore, F^- can influence both the reaction rate and turnover number. This biphasic kinetics was also observed at different ABTS concentrations (Figure S2)

The kinetics of TMB oxidation were next examined. With 5 mM F^-, the initial rate increased by ~200-fold by monitoring the absorbance at 652 nm (Figure 3B). Interestingly, with 5 mM F^-, the absorption at 652 nm decreased after 1 min and a yellowish product formed (#3 of inset). This was due to the further oxidation of the green one-electron oxidation intermediate to the yellow two-electron oxidation product (Figure S3). This can be followed at 450 nm (Figure S4). This fast formation of two-electron product strongly indicates the significantly enhanced catalytic activity of nanoceria after F^- capping.

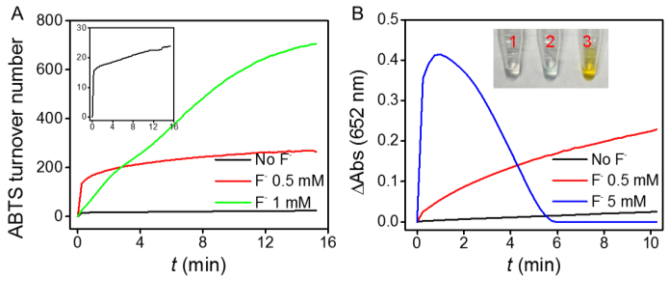

Figure 3. Effect of F^- on the kinetics of (A) ABTS (420 nm) and (B) TMB (652 nm) oxidation in the presence of nanoceria. Inset of (A): the F^- free sample at a smaller *y*-axis scale. Inset of (B): photographs of TMB after reacting with CeO_2 (1: no F^-; 2: 0.5 mM F^-; 3: 5 mM F^-).

A few mechanisms may explain the promoter effect of F^-: free radical generation, surface charge modulate, or facilitated electron transfer. First, the free radical mechanism was tested. For example, F^- capping enhanced the photo-oxidation activity of TiO_2,[36,38] which was attributed to the generation of free radicals. Terephthalic acid (TPA) is a commonly used fluorescent radical probe.[40] Oxidized TPA emits at 420 nm (Figure 4A, red trace). However, neither the naked nor the F^--treated nanoceria induced free radicals based on the lack of TPA fluorescence enhancement (Figure 4A). Therefore, the free radical mechanism is not supported.

Second, the surface charge of nanoceria was explored. The ζ-potential of nanoceria as a function of F^- concentration was measured (Figure 4B, red dots). At pH 4 (the reaction pH), nanoceria is positively charged due to protonation of its surface hydroxyl groups. The positively charged surface was retained until the F^- reached ~0.5 mM. After that, the surface positive charge diminished and became nearly neutral with 1 mM F^-. Further increase of F^- inverted the charge to negative. For comparison, the ζ-potential of nanoceria remained positive in the presence of Cl^- (blue squares), suggest a high affinity adsorption of F^-.

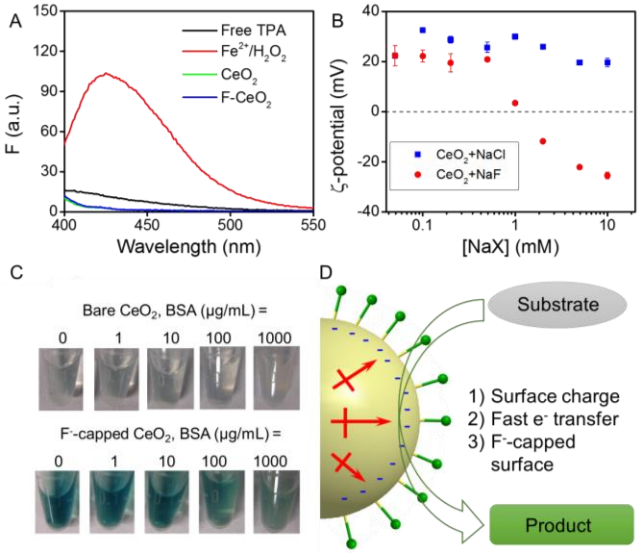

Figure 4. Mechanistic investigation of F^--capped nanoceria with enhanced oxidase activity. (A) Probing free radicals using TPA. Oxidized TPA emits at 420 nm and Fe^{2+}/H_2O_2 was used as a positive control. (B) ζ-potential of nanoceria (100 μg/mL) as a function of F^- and Cl^- concentration at pH 4 (acetate buffer, 20 mM). (C) Photographs of ABTS oxidatiaon by bare and F^--capped CeO_2 in the presence of various concentrations of BSA protein. (D) Proposed effects of F^- as a promoter for the CeO_2 nanozyme.

Such charge inversion after F^- adsorption may partially explain the oxidation kinetics of ABTS and TMB. Without F^-, the cationic nanoceria adsorbed negatively charged ABTS quickly. With 0.5 mM F^-, the surface remained positively charged, explaining the initial fast kinetics (Figure 3A, red trace) of ABTS oxidation. With 1 mM F^-, the surface became neutral or even slightly anionic, weakening the attraction to ABTS. Therefore, the initial rate was slower than that with 0.5 mM F^-. On the other hand, without F^-, oxidation of cationic TMB was very slow due to charge repulsion. As the surface became negative with F^-, the electrostatic repulsion became attraction for TMB, leading to over 200-fold rate increase. This electrostatic interaction mechanism was further supported by investigating the effect of ionic strength on the initial reaction rates (Figure S5). For example, for the F^--treated nanoceria, NaCl accelerated ABTS oxidation but inhibited TMB attributable to the charge screening effect of the added salt.

This simple surface charge model, however, cannot fully explain the rate enhancement. For example, nanoceria incubated with various surfactants (e.g. cationic CTAB, neutral Tween 80 and anionic SDS) failed to show such a rate enhancement (Figure S6). Therefore, beyond this simple electrostatic model, which only explains the initial substrate adsorption, other factors must also be important for the sustained turnover. For example, fluorinated surfaces have low surface energy and thus may decrease the affinity of the oxidation products. Product inhibition seems to be a main reason for the deactivation of the bare nanoceria. We also tested F^--capped CeO_2 in protein, and significant activity was still retained with up to 1 mg/mL

of bovine serum albumin (BSA). Another oxidase nanozyme, gold nanoparticles, however, is completely inhibited even at much lower BSA concentrations.[41]

In addition to sustained turnover, the reaction rates are also enhanced by F^-, suggesting that F^- might directly influence the oxidation reactions. This might be related to a previously proposed electron sponge mechanism for nanoceria.[42] In this mechanism, nanoceria as a whole particle (rather than individual surface sites) accepts and donates electrons. Since F^- is a strongly electron withdrawing ligand, it makes the nanoceria even more electron poor, and thus an even better electron sponge. Furthermore, F^--modified surfaces also facilitate O_2 adsorption.[43] Since O_2 is the actual oxidant in these reactions, F^- might help regenerate the catalyst as well. We summarized the roles of F^- in Figure 4D: 1) altering surface charge of nanoceria for tuning substrate adsorption affinity; 2) facilitating electron transfer between substrates, oxygen, and nanoceria; and 3) preventing product inhibition.

The above studies suggest that the effect of F^- is unique to its chemical properties, and the same may not happen with other anions. Thus it may allow a selective assay for F^- detection. Excessive F^- causes many adverse health effects (e.g., bone fractures, urolithiasis, and cancer).[44] Sensing F^- is an active research topic in the past few decades.[33] Traditional methods for F^- detection involve ion-chromatography and ion-selective electrodes, requiring sophisticated or fragile instruments and are not suitable for field F^- monitoring. Recently, optical sensors were developed based on F^- binding to the sensor molecules, F^--induced bond cleavage,[45-47] or nanomaterials.[48]

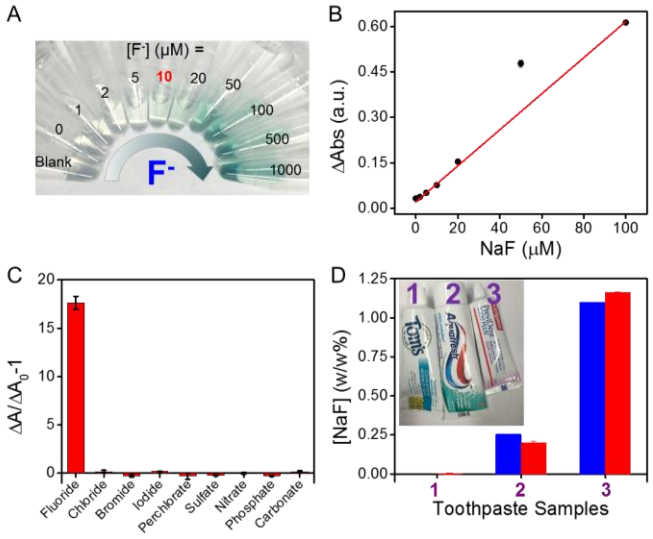

Figure 5. Detection of F^- using nanoceria and ABTS. (A) Photographs showing F^- concentration dependent sensor color change. (B) Sensor calibration curve using UV-vis spectrometry. (C) Selectivity test against various common anions. [F^-] = 0.1 mM; other anions 1 mM. (D) Detection of F^- in toothpastes. Inset: the photograph of the three toothpastes used. Blue bars: labeled fluoride content; red bars: fluoride measured by the sensor.

We mixed nanoceria with different concentrations of F^-. With more F^-, the color of ABTS was stronger. As low as 10 μM F^- can be determined by the naked eye (Figure 5A). The absorbance at 420 nm after 10 min reaction was measured by UV-vis spectroscopy to quantify the color intensity (Figure 5B). A linear range up to 100 μM F^- was obtained, after which the color started to saturate. The limit of detection (LOD) was calculated to be 0.64 μM based on 3σ/slope (σ = the standard deviation of the background variation). This LOD is over 100-fold lower than the guideline recommended by the World Health Organization (79 μM) for drinking water.

The selectivity was further tested (Figure 5C). Other common anions did not induce a significant enhancing effect of ABTS oxidation even at a 10-fold higher concentration. This high selectivity for F^- also supports it special chemical property to enable its promoter function for nanoceria. These studies support the feasibility of ABTS/nanoceria as a sensor for F^-. To test its application in real samples, Lake Huron water spiked with F^- was tested (Figure S8), and the response was very similar to that of the Milli-Q water.

Many toothpastes contain fluoride. Thus, we further challenged this F^- sensor with three toothpastes. To minimize the matrix effect, we used the standard addition method (Figure 5D, Figure S9). The F^- in sample 1 (F^--free) was lower than the detection limit of our sensor (0.000496%), consistent with its lack of fluoride as indicated by the vendor. We obtained 0.198% (w/w) of F^- in sample 2 (a normal toothpaste), which is ~80% of the labeled concentration (0.254%). Finally, the high F^- sample 3 was also very close to the labeled content.

Methods

Chemicals. Nanoceria dispersion (catalog number 289744, 20 wt % dispersed in 2.5% acetic acid), H_2O_2 solution (30 wt %) 3,3',5,5'-tetramethylbenzidine (TMB), 2,2'-azino-bis(3-ethylbenzothiazoline-6-sulfonic acid) diammonium salt (ABTS), terephthalic acid (TPA), sodium sulfate, and surfactants (sodium dodecyl sulfate (SDS), hexadecyl trimethyl ammonium bromide (CTAB), and Tween 80) were purchased form Sigma-Aldrich. Sodium fluoride, sodium chloride, sodium bromide, sodium iodide, sodium nitrate, sodium bicarbonate, sodium acetate, sodium phosphate dibasic heptahydrate, sodium perchlorate and 4-(2-hydroxyethyl) piperazine-1-ethanesulfonic acid (HEPES) were from Mandel Scientific (Guelph, ON, Canada). Toothpastes were purchased from a local supermarket. Milli-Q water was used for all of the experiments. *Transmission Electron Microscopy (TEM), Dynamic Light Scattering (DLS) and UV-vis Spectroscopy*. The morphology and size of nanoceria were investigated by TME measurement (Philips CM10). The TEM samples were prepared by dropping nanoceria dispersion (10 μg/mL) into a copper grid and were allowed to dry overnight at room temperature. The UV-vis spectra were scanned after mixing nanoceria with ABTS using a UV-vis spectrometer (Agilent 8453A). The visual images were taken by a digital camera. The hydrodynamic size and surface charge of nanoceria were measured using DLS (Malvern Nanosizer ZS90). Typically, 100 μg/mL of nanoceria was dispersed in water for size measurements and in buffer solution (acetate buffer, pH 4, 20 mM) for ζ-potential measurements. Anions were incubated with nanoceria for 10 min before measurement.

Kinetic measurements of ABTS or TMB oxidation. Typically, nanoceria (100 μg/mL) was dispersed in 100 μL of acetate buffer (pH 4, 20 mM) containing fluoride at designed concentrations. After 10 min incubation, 1 μL of concentrated substrates (ABTS or TMB) was introduced to initiate the reaction. The absorbance at 420 nm for

ABTS, or at 450 nm and 650 nm for TMB were monitored by a mircroplate reader.

Effect of NaCl and BSA on oxidation kinetics. Nanoceria (100 μg/mL) was respectively incubated with three concentrations of fluoride (0, 0.5 mM, and 5 mM) at different NaCl concentrations (0, 50, 150, and 300 mM) in acetate buffer (pH 4, 20 mM). After adding ABTS (0.5 mM) and a quick mixing, the absorbance at 420 nm was monitored for 10 min. To test the effect of BSA, bare nanoceria (100 μg/mL) or fluoride capped nanoceria was incubated with various concentrations of BSA for 15 min. The images were taken after adding ABTS (0.5 mM) for 20 min.

TPA Assay. Nanoceria (100 μg/mL) was incubated with TPA (0.5 mM) with or without fluoride (1 mM) at pH 4 (acetate buffer, 20 mM) for 30 min. The pH was then adjusted to around 7 by adding NaOH. The fluorescence of TPA was monitored by exciting at 310 nm. As a control, Fenton agent (Fe^{2+} 0.5 mM, H_2O_2 10 mM) was used to induce the TPA oxidation.

Detection of fluoride. Detection of fluoride in buffer solution was performed by adding various concentrations of fluoride to nanoceria (40 μg/mL) in an acetate buffer (pH 4, 20 mM) (solution A). ABTS (1 mM) was dissolved in the same buffer (solution B). After a quick mixing of solution A and B (50 μL for each), the absorbance at 420 nm was monitored. The selectivity of fluoride detection was carried out in a similar way. To achieve fluoride detection in Lake water, water from Lake Huron was used as a matrix. A small volume of concentrated buffer, fluoride, nanoceria, and ABTS was sequentially added to the Lake water. To detect fluoride in toothpaste, toothpaste was first dispersed in Milli-Q water (5%). The dispersion was further diluted to make sure the final concentration of NaF was in the linear range of the sensor system. Then, a similar procedure as fluoride detection in buffer was carried out using the standard addition method.

Conclusions

In summary, this work reveals the importance of surface chemistry on a model nanozyme, pushing the nanozyme performance approaching true enzymes. The oxidase activity of nanoceria was drastically promoted by F^- capping: 1) the acitivty is increased over 100-fold; 2) more importantly, unlike the naked nanoceria, which is quickly deactivated within 1 min, the fluoride-capped nanoceria retains efficient turnover over a much longer time. This activity modulation was attributed to electrostatic interactions, reduced surface energy, and facilitated electron transfer. Detection of fluoride in lake water and toothpastes was demonstrated with excellent sensitivity and specificity. We believe this surface engineering approach can also be applied to other nanozymes (may not be fluoride in all cases) to push for practical applications. By such research, our fundamental insights into nanoscale surfaces is significantly enhanced.

Acknowledgement

Funding for this work is from the Natural Sciences and Engineering Research Council of Canada (NSERC).

Notes and references

1. L. Gao, J. Zhuang, L. Nie, J. Zhang, Y. Zhang, N. Gu, T. Wang, J. Feng, D. Yang, S. Perrett and X. Yan, *Nat. Nanotechnol.*, 2007, **2**, 577-583.
2. H. Wei and E. Wang, *Chem. Soc. Rev.*, 2013, **42**, 6060-6093.
3. H. Wei and E. Wang, *Anal. Chem.*, 2008, **80**, 2250-2254.
4. Y. Lin, J. Ren and X. Qu, *Adv. Mater.*, 2014, **26**, 4200-4217.
5. C. Xu and X. Qu, *NPG Asia Mater.*, 2014, **6**, e90.
6. N. A. Kotov, *Science*, 2010, **330**, 188-189.
7. Y. Lin, J. Ren and X. Qu, *Acc. Chem. Res.*, 2014, **47**, 1097-1105.
8. X. Zheng, Q. Liu, C. Jing, Y. Li, D. Li, W. Luo, Y. Wen, Y. He, Q. Huang, Y.-T. Long and C. Fan, *Angew. Chem. Int. Ed.*, 2011, **50**, 11994-11998.
9. W. Luo, C. Zhu, S. Su, D. Li, Y. He, Q. Huang and C. Fan, *ACS Nano*, 2010, **4**, 7451-7458.
10. Y. Song, K. Qu, C. Zhao, J. Ren and X. Qu, *Adv. Mater.*, 2010, **22**, 2206-2210.
11. H. Sun, A. Zhao, N. Gao, K. Li, J. Ren and X. Qu, *Angew. Chem. Int. Ed.*, 2015, **54**, 7176-7180.
12. B. Liu and J. Liu, *Nanoscale*, 2015, **7**, 13831-13835.
13. D. Duan, K. Fan, D. Zhang, S. Tan, M. Liang, Y. Liu, J. Zhang, P. Zhang, W. Liu, X. Qiu, G. P. Kobinger, G. Fu Gao and X. Yan, *Biosens. Bioelectron.*, 2015, **74**, 134-141.
14. M. Liang, K. Fan, Y. Pan, H. Jiang, F. Wang, D. Yang, D. Lu, J. Feng, J. Zhao, L. Yang and X. Yan, *Anal. Chem.*, 2013, **85**, 308-312.
15. K. Fan, C. Cao, Y. Pan, D. Lu, D. Yang, J. Feng, L. Song, M. Liang and X. Yan, *Nat. Nanotechnol.*, 2012, **7**, 459-464.
16. C. Xu, Z. Liu, L. Wu, J. Ren and X. Qu, *Adv. Funct. Mater.*, 2014, **24**, 1624-1630.
17. R. Pautler, E. Y. Kelly, P.-J. J. Huang, J. Cao, B. Liu and J. Liu, *ACS Appl. Mater. Interfaces*, 2013, **5**, 6820-6825.
18. B. Liu, Z. Sun, P.-J. J. Huang and J. Liu, *J. Am. Chem. Soc.*, 2015, **137**, 1290-1295.
19. A. A. Vernekar, T. Das, S. Ghosh and G. Mugesh, *Chemistry – An Asian Journal*, 2016, **11**, 72-76.
20. A. Asati, S. Santra, C. Kaittanis, S. Nath and J. M. Perez, *Angew. Chem., Int. Ed.*, 2009, **48**, 2308-2312.
21. X. Liu, Q. Wang, H. Zhao, L. Zhang, Y. Su and Y. Lv, *Analyst*, 2012, **137**, 4552-4558.
22. K. Zhang, X. Hu, J. Liu, J.-J. Yin, S. Hou, T. Wen, W. He, Y. Ji, Y. Guo, Q. Wang and X. Wu, *Langmuir*, 2011, **27**, 2796-2803.
23. C.-J. Yu, T.-H. Chen, J.-Y. Jiang and W.-L. Tseng, *Nanoscale*, 2014, **6**, 9618-9624.
24. T. Pirmohamed, J. M. Dowding, S. Singh, B. Wasserman, E. Heckert, A. S. Karakoti, J. E. S. King, S. Seal and W. T. Self, *Chem. Commun.*, 2010, **46**, 2736-2738.
25. N. P. Sardesai, D. Andreescu and S. Andreescu, *J. Am. Chem. Soc.*, 2013, **135**, 16770-16773.
26. C. Korsvik, S. Patil, S. Seal and W. T. Self, *Chem. Commun.*, 2007, 1056-1058.
27. Y. Li, X. He, J.-J. Yin, Y. Ma, P. Zhang, J. Li, Y. Ding, J. Zhang, Y. Zhao, Z. Chai and Z. Zhang, *Angew. Chem. Int. Ed.*, 2015, **54**, 1832-1835.
28. M. H. Kuchma, C. B. Komanski, J. Colon, A. Teblum, A. E. Masunov, B. Alvarado, S. Babu, S. Seal, J. Summy and C. H. Baker, *Nanomedicine: NBM*, 2010, **6**, 738-744.
29. I. Celardo, M. De Nicola, C. Mandoli, J. Z. Pedersen, E. Traversa and L. Ghibelli, *ACS Nano*, 2011, **5**, 4537-4549.
30. X. Liu, K. Zhou, L. Wang, B. Wang and Y. Li, *J. Am. Chem. Soc.*, 2009, **131**, 3140-3141.
31. A. Asati, C. Kaittanis, S. Santra and J. M. Perez, *Anal. Chem.*, 2011, **83**, 2547-2553.
32. R. N. McCormack, P. Mendez, S. Barkam, C. J. Neal, S. Das and S. Seal, *J. Phys. Chem. C*, 2014, **118**, 18992-19006.
33. Y. Zhou, J. F. Zhang and J. Yoon, *Chem. Rev.*, 2014, **114**, 5511-5571.
34. F. Karlický, K. Kumara Ramanatha Datta, M. Otyepka and R. Zbořil, *ACS Nano*, 2013, **7**, 6434-6464.

35. H. Sun, H. Ji, E. Ju, Y. Guan, J. Ren and X. Qu, *Chem. – Eur. J.*, 2015, **21**, 3791-3797.
36. M. Mrowetz and E. Selli, *Phys. Chem. Chem. Phys.*, 2005, **7**, 1100-1102.
37. H. Park and W. Choi, *J. Phys. Chem. B*, 2004, **108**, 4086-4093.
38. C. Minero, G. Mariella, V. Maurino and E. Pelizzetti, *Langmuir*, 2000, **16**, 2632-2641.
39. S. Ahmad, K. Gopalaiah, S. N. Chandrudu and R. Nagarajan, *Inorg. Chem.*, 2014, **53**, 2030-2039.
40. K.-i. Ishibashi, A. Fujishima, T. Watanabe and K. Hashimoto, *J. Photochem. Photobiol., A*, 2000, **134**, 139-142.
41. N. J. Lang, B. Liu and J. Liu, *J. Colloid Interf. Sci.*, 2014, **428**, 78-83.
42. J.-D. Cafun, K. O. Kvashnina, E. Casals, V. F. Puntes and P. Glatzel, *ACS Nano*, 2013, **7**, 10726-10732.
43. Y. Luan, L. Jing, Y. Xie, X. Sun, Y. Feng and H. Fu, *ACS Catal.*, 2013, **3**, 1378-1385.
44. E. T. Everett, *J. Dent. Res.*, 2011, **90**, 552-560.
45. C.-W. Chiu and F. P. Gabbaï, *J. Am. Chem. Soc.*, 2006, **128**, 14248-14249.
46. S. Guha and S. Saha, *J. Am. Chem. Soc.*, 2010, **132**, 17674-17677.
47. T. W. Hudnall and F. P. Gabbaï, *J. Am. Chem. Soc.*, 2007, **129**, 11978-11986.
48. H. Wang, P.-H. Fan, B. Tong, Y.-P. Dong, X.-M. Ou, F. Li and X.-H. Zhang, *Adv. Funct. Mater.*, 2015, **25**, 1506-1510.